Pergamon

Cement and Concrete Research 29 (1999) 1969–1976

CEMENT AND CONCRETE RESEARCH

Resistance of sodium polyphosphate-modified fly ash/calcium aluminate blend cements to hot H_2SO_4 solution

Toshifumi Sugama[a,*], Lawrence Weber[b], Lance E. Brothers[c]

[a]*Materials and Chemical Sciences Division, Department of Applied Science, Brookhaven National Laboratory, Upton, NY 11973, USA*

[b]*Unocal Corporation, 1414 Southwest Freeway, Sugar Land, TX 77478, USA*

[c]*Halliburton Energy Services, 2600 S. 2nd Street, Duncan, OK 73536-0442, USA*

Received 25 February 1999; accepted 12 October 1999

Abstract

Sodium polyphosphate-modified Class F fly ash/calcium aluminate blend (SFCB) cements were prepared at room temperature and their resistance to hot acid erosion was evaluated by submerging them in H_2SO_4 solution (pH 1.6) at 90°C. Sodium polyphosphate preferentially reacted with calcium aluminate cement (CAC) to form amorphous $Ca(HPO_4).xH_2O$ and $Al_2O_3.xH_2O$ gel, rather than fly ash. These amorphous reaction products, which bound the partially reacted and unreacted CAC and fly ash particles into a coherent mass, were responsible for strengthening and densifying the SFCB specimens at room temperature, playing an essential role in mitigating their acid erosion. In these cements, the extent of acid erosion depended primarily on the ratio of fly ash/CAC; namely, those with a higher ratio underwent a severe erosion. This effect was due to the formation of a porous structure, which allowed acid to permeate the cement easily, diminishing the protective activity of $Ca(HPO_4).xH_2O$ and $Al_2O_3.xH_2O$ gel against H_2SO_4.

Keywords: Calcium phosphate cement; Sulfate attack; Fly ash; Calcium aluminate cement; Sodium polyphosphate; Geothermal cement

1. Introduction

In dealing with the problem of carbonation-caused disintegration of cementitious materials used for completing geothermal wells containing a highly concentrated CO_2 of >10,000 ppm at temperatures up to 300°C, we successfully formulated a high-temperature CO_2-resistant hydrothermal cement. This cement was prepared by an acid-base reaction between sodium polyphosphate as an acid liquid and Class F fly ash-blended calcium aluminate cement as a base powder reactant, followed by hydrothermal treatments at temperatures up to 300°C [1,2]. This cement synthesized by two-step reaction pathways, acid-base and hydrothermal reactions, was composed of two major crystalline phases, hydroxyapatite (HOAp) and analcime (AN). When it was exposed for 6 months to hydrothermal brine solution containing ~40,000 CO_2 ppm at 300°C, the AN phase underwent a carbonation reaction to form the cancrinite (CAN) phase. Despite some loss in strength of the specimens caused by the AN → CAN phase transformation, there was no formation of HOAp-related carbonation phases, nor were calcium carbonate and calcium bicarbonate in the cements.

The technology for making this sodium polyphosphate-modified fly ash/calcium aluminate blend (SFCB) cement was transferred to two industrial collaborators, Unocal and Halliburton. Subsequent field testing and further development of the SFCB cement system by them led to a full-scale tests and a field-workable cement which was first emplaced by Unocal in a geothermal well in northern Sumatra, Indonesia, in September 1997. The pumping operation of cement in these wells, which was performed under the following conditions: bottomhole depth of 1680 m, downhole temperature of 280°C, and CO_2 concentration of 10,000 ppm, was very successful [3]. However, one question raised concerned the resistance of SFCB cements to highly concentrated H_2SO_4 environments (pH < 2.0) encountered in the well's surface ground water at low temperatures around 90°C. In response to this important concern, the objective of the present study was to investigate the susceptibility of SFCB cements to the reaction with H_2SO_4 solution at 90°C. The factors to be investigated were as follows: (1) the identification of phases formed in the exposed cements and their transformations; (2) the exploration of microstructure developed in the exposed cements; and (3) the changes in

* Corresponding author. Tel.: 516-344-4029; fax: 516-344-2359.
E-mail address: sugama@bnl.gov (T. Sugama)

0008-8846/99/$ – see front matter
PII: S0008-8846(99)00220-3

weight, compressive strength, and porosity of the specimens as a function of exposure time.

2. Experimental

2.1. Materials

Class F fly ash with a Blaine fineness of 10,585 cm^2/g was supplied by Pozament Corp., Indonesia; a typical analysis made in accordance with Spec. ASTM 618, showed 38.57 wt% silica, 38.57 wt% aluminum oxide, 11.95 wt% iron oxide, 1.36 wt% magnesium oxide, 1.94 wt% sulfur trioxde, 1.52 wt% sodium oxide, 0.47 wt% calcium oxide, and 1.94 wt% potassium oxide, with a 3.68 wt% loss on ignition at 816°C. The X-ray powder diffraction (XRD) data showed that the crystalline components of fly ash consist of two major phases, mullite and quartz. Commercial calcium aluminate cement (CAC, Refcon) obtained from Lehigh Cement Company, USA, was used to blend with the fly ash. The chemical constituents of this CAC are as follows; 57.4 wt% Al_2O_3, 1.2 wt% Fe_2O_3, 34.2 wt% CaO, 5.7 wt% SiO_2, 0.36 wt% SO_3, and 1.14 wt% other. CAC has three major phases, gehenite ($2CaO.Al_2O_3.SiO_2$, C_2AS), monocalcium aluminate ($CaO.Al_2O_3$, CA), and calcium dialuminate ($CaO.2Al_2O_3$, CA_2). A 25 wt% sodium polyphosphate [-(-$NaPO_3$-)-$_n$, NaP] supplied by the Aldrich Chemical Company Inc., USA, was employed as the cement-forming aqueous reactant to modify the CAC-blended fly ash solid reactants. In this study, the composition of the solid reactants, made up in a Twin Shell Dry Blender, had the ratios of fly ash/CAC of 80/20, 60/40, 40/60, and 20/80 by weight.

Cement slurries of the formulations shown in Table 1 were prepared by handmixing a certain amount of fly ash-blended CAC and 40 wt% (25 wt% NaP solution) for the SFCB cement systems. These cement slurries were then cast into cylindrical molds (30 mm diam. × 60 mm long) and allowed them to harden for 24 hours at room temperature. These aged specimens were left for 24 hours in air oven at 110°C, allowing them to eliminate any free water from the specimens. The dried specimens were exposed for up to 25 days to the H_2SO_4 solution with pH 1.6 at 90°C; subsequently, we explored the alterations in microstructure caused by the acid erosion and identified the amorphous and crystalline phase compositions and transformations. All data were correlated directly with the loss in weight, compressive strength, and porosity of the eroded specimens.

2.2. Measurements

To measure the pH of the pore solutions of SFCB slurries with different fly ash/CAC ratios, the aqueous samples were prepared in the following sequence. First, 120-g fly ash-CAC mixture was throughly mixed with 40 g of a 25 wt% NaP solution, and agitated for 3 minutes with a shear-blend mixer at room temperature. The pore solution was then extracted by centrifugal separation. XRD and Fourier Transform Infrared Spectroscopy (FT-IR) were used to identify the phase composition formed in these cement specimens before exposure, and to gain information on the transformation of phases caused by the exposure to the H_2SO_4 solution with pH 1.6 at 90°C. Scanning electron microscopy (SEM) coupled with energy-dispersive X-ray spectrometry (EDX) was employed to explore the microstructure developed in the specimens after exposure, and to detect its chemical components. Compressive strength tests were made on neat cement specimens with a diameter of 30 mm and a length of 60 mm; the result given is the average value from three specimens. The porosity of cement specimens was determined by helium comparison pyconometry.

3. Results and discussion

Table 2 compares the pH values of the pore solutions extracted from the cement slurries which were prepared by varying the proportion of fly ash to CAC. The pH value of cement-forming NaP liquid reactant as control was 6.06, representing a very mild acid. The creation of this mild acid by dissolving NaP granules in an aqueous medium might be due to an exchange of Na^+ ions in the NaP molecule for H^+ ions in water, thereby resulting in the dissociation of HPO_4^{2-} ions from the NaP [4]. When the NaP solution was added to the blended solid reactant with fly ash/CAC ratio of 80/20, the pH rose 3.3% to 6.26. The data showed that the pH value depended mainly on the fly ash/CAC ratio; there was an increase in pH value with a decreasing its ratio. In other words, a large proportion of CAC to fly ash in the blended solid reactant resulted in the increase in the pH of the cement slurries; accordingly, the slurry made with 20/80 ratio was almost neutral. As is well known [5,6], the Ca^{2+} ion is one of the ionic species which act to neutralize HPO_4^{2-} acid. Since the main chemical constituents of fly ash are Al_2O_3 and SiO_2, it is possible to assume that the Ca^{2+} liberated from CAC in the NaP solution plays a major role in increasing the pH of the slurries. The reaction between Ca^{2+}

Table 1
Formulations of fly ash-calcium aluminate-sodium polyphosphate cement slurries

Fly ash/CAC ratio	Fly ash, wt%	CAC, wt%	25 wt% NaP, wt%
80/20	48	12	40
60/40	36	24	40
40/60	24	36	40
20/80	12	48	40

Table 2
The pH of pore solution in cement slurry

Fly ash/CAC ratio	pH
NaP solution	6.06
80/20	6.26
60/40	6.32
40/60	6.59
20/80	6.8

and HPO_4^{2-} in an aqueous medium may lead to the formation of $Ca(HPO_4).xH_2O$ [7].

The SFCB slurry specimens made with fly ash/CAC ratios of 80/20, 60/40, 40/60, and 20/80 were left for 24 hours at room temperature to harden, and then dried for 24 hours in an oven at 110°C. The dried specimens were exposed for up to 25 days to a H_2SO_4 solution at 90°C. After exposure, we recorded the loss in weight as a function of the exposure time (Fig. 1). All the specimens lost weight to different degrees, and the loss became greater with the extension of exposure time; in particular, the specimens made with 80/20 ratio underwent a severe acid erosion after exposure for only 5 days. Thus, no further exposure tests of this specimen were conducted because of its disintegration. The data clearly showed that a decrease in the proportion of fly ash/CAC in this cement system tends to reduce the degree of loss in weight. Thus, as an excessive amount of fly ash is added to the CAC, the specimens become more susceptible to acid erosion. In fact, the effectiveness of fly ash/CAC ratio in minimizing the acid erosion is ranked as follows: 20/80 > 40/60 > 60/40 > 80/20.

To understand the mechanism of H_2SO_4 attack on the SFCB cements, the crystalline phase composition and transformation for these specimens before and after exposure was investigated by XRD, ranging from 0.249 to 0.444 nm. The results from these specimens are given in Figs. 2 and 3. For the unexposed specimens (Fig. 2), the all d-spacings of the 80/20 ratio specimen (Fig. 2a) were related directly to the fly ash- and CAC-related crystalline phases; the quartz (SiO_2) and mullite ($3Al_2O_3.2SiO_2$) in the fly ash and the C_2AS, CA, and CA_2 in the CAC. No d-spacings for the reaction products as crystalline phases were detected in this diffraction pattern. Similarly, no reaction products were found from the XRD patterns of the 40/60 (Fig. 2b) and 20/80 (Fig 2c) ratio specimens. As expected, the feature of these diffraction patterns showed the presence of the CAC-related phases coexisting with quartz. However, it was very difficult to identify the mullite-associated d-spacings because of the interference of strong C_2AS- and CA-related lines. Nevertheless, it is apparent that these specimens cured for 24 hours at room temperature do not form any crystalline reaction products. Hence, the reaction products, which bind the par-

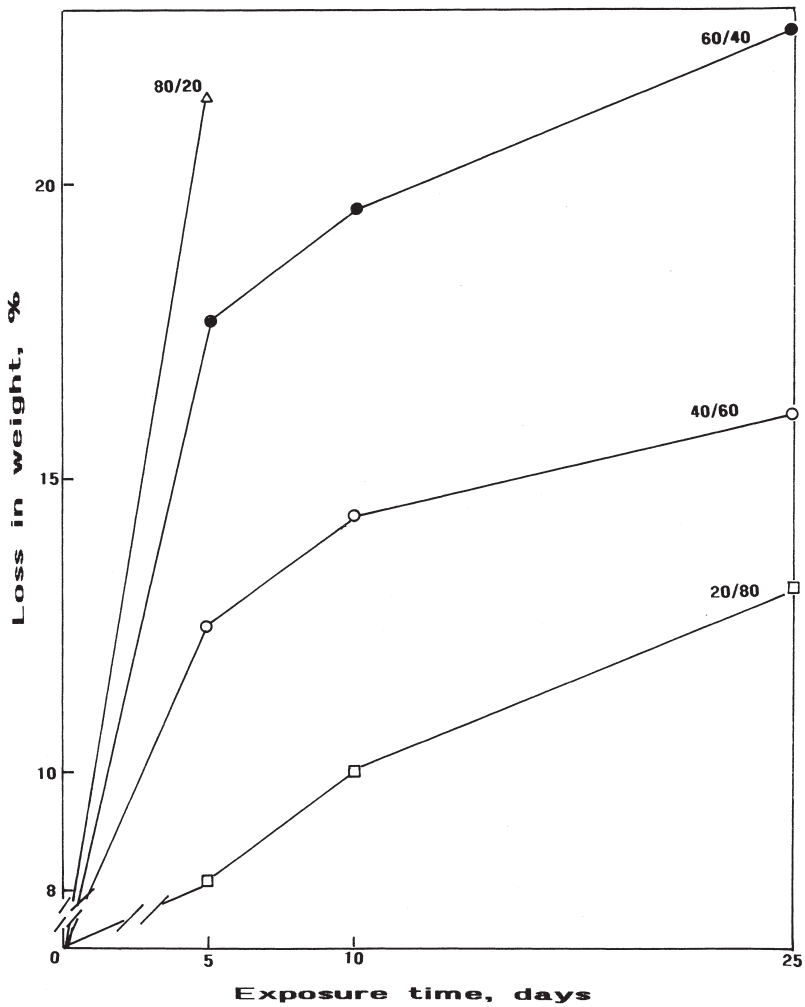

Fig. 1. Loss in weight for 80/20, 60/40, 40/60, and 20/80 fly ash/CAC ratio cements after exposure for up to 25 days to H_2SO_4 solution (pH 1.6) at 90°C.

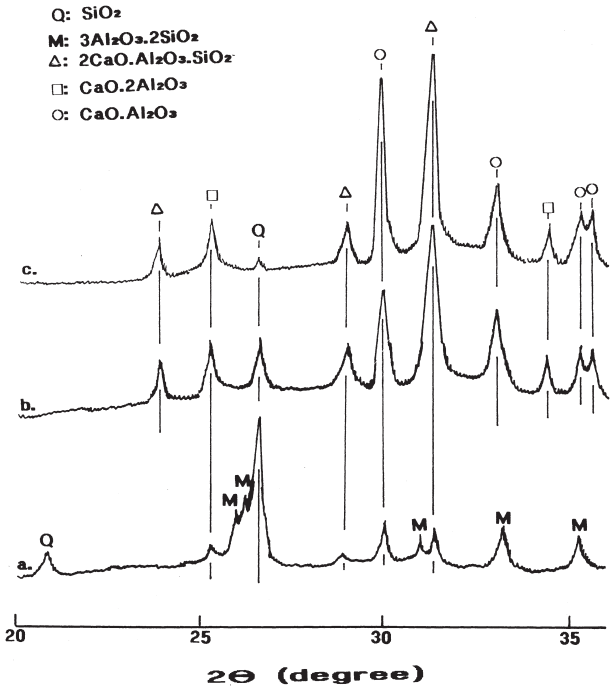

Fig. 2. XRD patterns of the specimens made with (a) 80/20, (b) 40/60, and (c) 20/80 fly ash/CAC ratios at room temperature.

tially reacted and unreacted fly ash and CAC particles into a coherent mass, are thought to be essentially amorphous.

To substantiate the formation of amorphous reaction products, focus centered on identifying their compounds by FT-IR. Fig. 3 illustrates FT-IR spectra over the frequency range from 1600 to 600 cm^{-1} for these SFCB specimens before exposure to H_2SO_4, and the NaP, fly ash, and CAC powder reactants as reference samples. The NaP reference sample was prepared by drying a 25 wt% solution for 24 hours in an oven at 110°C. The spectral feature of NaP (Fig. 3a) represents the typical sodium dibasic phosphate structure [8], reflecting the stretching vibration of the P=O double bond at 1302 and 1160 cm^{-1}, ionic P-O stretching vibration at the peaks of 1049 and 979 cm^{-1}, and bending vibration of P-O-H bands at 932 cm^{-1}. This information seems to demonstrate that once NaP is dissolved in an aqueous medium, its linear metaphosphate structure as a polymorphism might be transferred in the dibasic orthophosphate structure by the bond breakage of P-O-P chain in the polyphosphate. In fact, there was no band near 850 cm^{-1}, originating from the P-O-P linkage. The spectrum of fly ash (Fig. 3b) had the mullite- and quartz-related bands at 1090 and 791 cm^{-1}. The three vibration bands at 1020, 803, and 640 cm^{-1} for the CAC reactant (Fig. 3c) are assignable to three aluminates, C_2AS, CA, and CA_2. By comparison with those of these reference samples, no particular feature of the spectrum was observed from the 80/20 ratio SFCB specimens (Fig. 3d). When the solid reactant with a fly ash/CAC ratio of 60/40 was incorporated into the NaP solution, the spectral features were quite different from those of the 80/

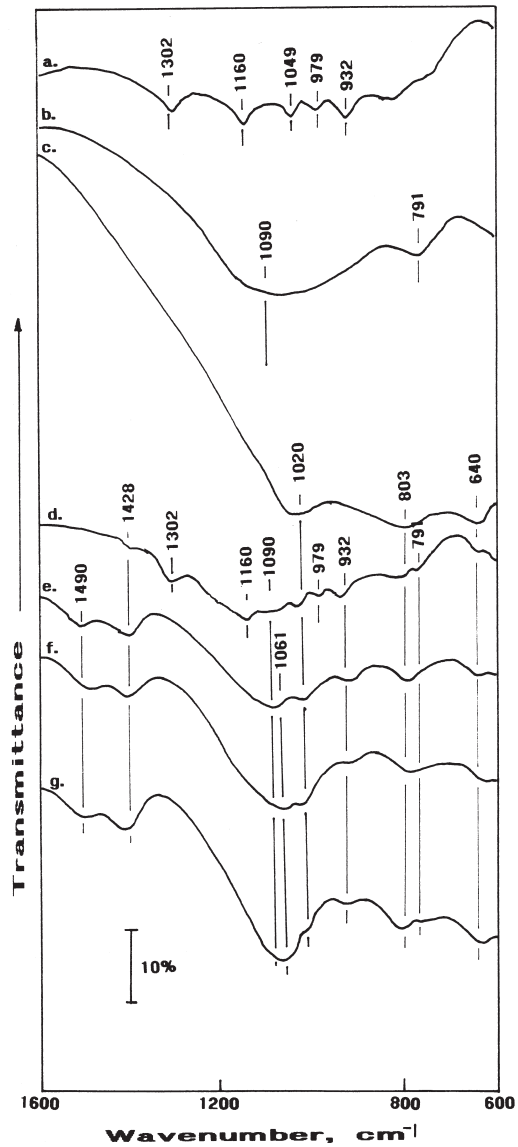

Fig. 3. FT-IR spectra for (a) NaP, (b) fly ash, and (c) CAC as reference samples, and (d) 80/20, (e) 60/40, (f) 40/60, and (g) 20/80 ratio specimens before exposure to acid.

20 ratio samples. The differences were as follows: (1) the elimination of frequency bands at 1302 and 1160 cm^{-1} originating from P=O double bonds, and (2) the emergence of new bands at 1490, 1428, and 1061 cm^{-1}. Since the formation of carbonate compounds can be identified from the bands in the range 1490–1410 cm^{-1} [9], the contributors to new bands at 1428 and 1490 cm^{-1} were, respectively, the CO_3 in the calcite, and other carbonates that differed from the calcite. Relating this to finding (1), the new band at 1061 cm^{-1} perhaps belongs to the P-O stretching mode in the formation of calcium dibasic phosphate hydrate, $Ca(HPO_4).xH_2O$ [9], having a tetrahedral PO_4 structure yielded by the rupture of P=O bonds in NaP. Although not shown in the figure, the spectrum of this sample indicated the presence of a strong peak at 3450 cm^{-1}, revealing the

O-H stretching in its hydrates. Assuming that our interpretation of these IR bands is valid, the $Ca(HPO_4).xH_2O$ as the amorphous phase was formed by the reaction between the Ca^{2+} cations liberated from CAC and the HPO_4^{2-} anions from NaP; $Ca^{2+} + HPO_4^{2-} + xH_2O \rightarrow Ca(HPO_4).xH_2O$. Since the uptake of Ca by NaP leaves Ca-destitute CAC surfaces, we assumed that the $Al_2O_3.xH_2O$ gel might be formed through the decalcification-hydration process of CAC [10]. However, it was difficult to identify $Al_2O_3.xH_2O$-related absorption bands near 800 and 650 cm^{-1} because of the interference of the bands related to other chemical compounds [11]. Since these amorphous $Ca(HPO_4).xH_2O$ and $Al_2O_3.xH_2O$ gel phases conceivably may bind partially reacted and unreached fly ash and CAC particles into a coherent mass, we assumed that these reaction products are responsible for strengthening and densifying the cement specimens. In fact, the 60/40 ratio specimens had a compressive strength of 14.3 MPa, and a porosity of 42.0%, corresponding to ~18% higher and ~19.7% lower, respectively, than those of the 80/20 ratio. Furthermore, the intensity of these new bands tends to be enhanced when the proportion of fly ash to CAC is reduced, seemingly manifested that more incorporation of CAC into the SFCB cement system not only leads to the formation of a substantial amount of the $Ca(HPO_4).xH_2O$ and $Al_2O_3.xH_2O$ gel reaction products, but also increases the rate of carbonation, especially for the calcite which may be formed by carbonation of unreacted CAC. However, despite enhancing the degree of carbonation, the increased amount of these reaction products in the cement bodies offered improved strength and reduced porosity of the specimens, reflecting a compressive strength of 16.4 MPa and 17.1 MPa, and a porosity of 38.4% and 36.2% for the 40/60 and 20/80 ratios, respectively. The data also manifested that incorporating a large amount of fly ash into the SFCB cement system causes a decline of compressive strength because of a poor reactivity of fly ash with NaP at room temperature.

Fig. 4 depicts the XRD patterns of the specimens after exposure to a hot acid solution. Comparing these with those before exposure, among the characteristics of the XRD tracing for the 80/20 ratio specimens (Fig. 4a) were (1) the appearance of new d-spacings related to the gypsum ($CaSO_4.2H_2O$); (2) the disappearance of two major chemical components, CA and CA_2, in CAC; and (3) the retention of a strong line intensity of unreacted fly ash. Relating to findings (1) and (2), a possible interpretation for the formation of gypsum with loss of CA and CA_2 is that the Ca in CA or CA_2 reacted with H_2SO_4 to precipitate gypsum. In fact, the line intensity of gypsum-related d-spacings increasingly enhanced when the proportion of fly ash to CAC was reduced. Again, no CA and CA_2 phases were detected in the 60/40, 40/60, and 20/80 ratio specimens, suggesting that the amount of gypsum formed depended mainly on the amount of unreacted CAC in the SFCB cement systems. In addition, not only does the reaction between H_2SO_4 and CA or CA_2 form gypsum, but it may be responsible for the formation of $Al_2O_3.xH_2O$ gel due to the decalcification of CA and CA_2; CaO. $Al_2O_3 + CaO.2Al_2O_3 + 2H_2SO_4 + xH_2O \rightarrow 2CaSO_4.2H_2O + 3Al_2O_3.xH_2O$. If there is such a reaction pathway, the boehmite, γ-AlOOH, which was identified in these patterns, might be formed by direct or indirect phase transition of $Al_2O_3.xH_2O$ gel. The $Al_2O_3.xH_2O \rightarrow$ γ-AlOOH phase transition generated during exposure seems to be evidence that the $Al_2O_3.xH_2O$ has little, if any susceptibility to the reaction with H_2SO_4. Since $Al_2O_3.xH_2O$ gel acts as the binder, this serves in protecting the cement against the acid erosion. A further increase in the height of the gypsum-related line intensity can be seen from the 20/80 ratio specimens, reflecting the generation of massive amounts of gypsum during exposure. No ettringite phase, which is formed by a reaction between hydrated aluminate and gypsum, was found in these patterns.

This information was supported by inspecting the FT-IR spectra for the same specimens as used in the XRD study. Fig. 5 shows the spectra for these exposed specimens over the frequency range of 1600 to 600 cm^{-1}. By comparison with that before exposure, the spectrum of the exposed 80/20 ratio specimens showed the two noticeable differences: (1) the elimination of all the CAC- and NaP-related absorption bands, while the band at 791 cm^{-1}, belonging to the fly

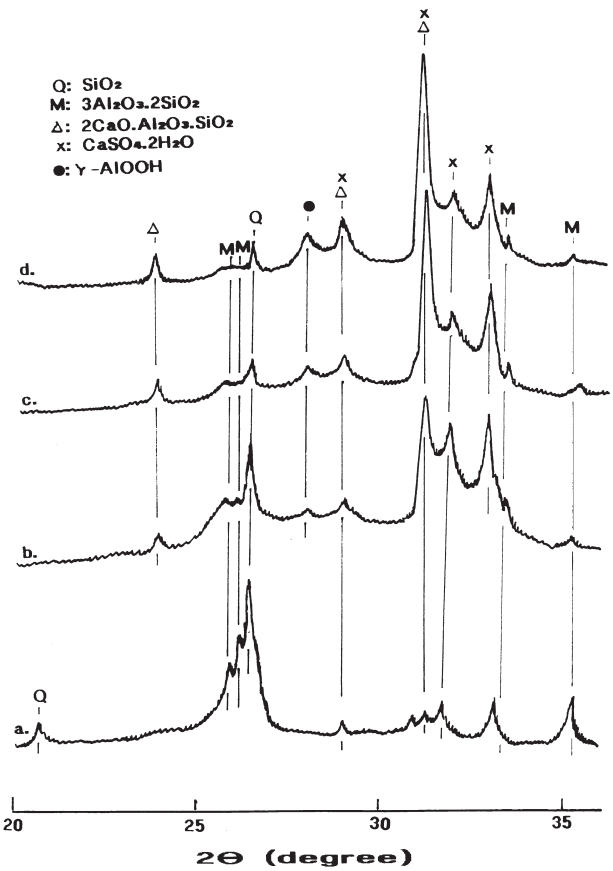

Fig. 4. XRD tracings for (a) 80/20, (b) 60/40, (c) 40/60, and (d) 20/80 ratio specimens after exposure to acid.

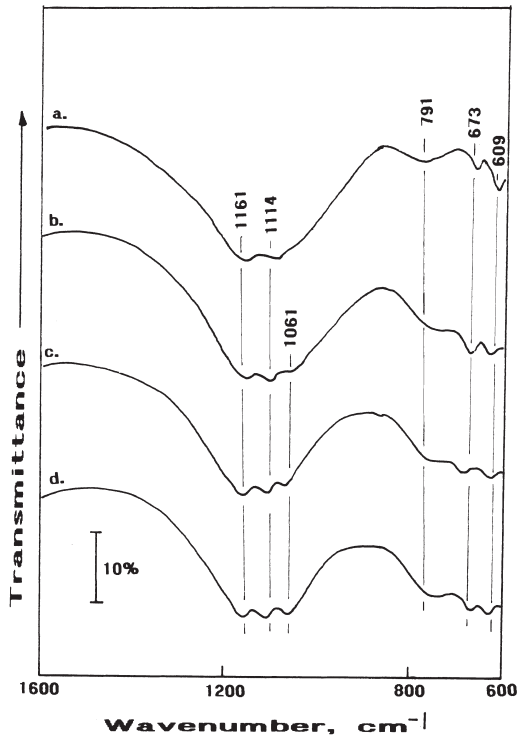

Fig. 5. FT-IR spectra for (a) 80/20, (b) 60/40, (c) 40/60, and (d) 20/80 ratio specimens after exposure to acid.

ash and $Al_2O_3.xH_2O$ gel, still remains; and (2) the growth of new bands at 1161, 1114, 673, and 609 cm^{-1}. According to the literature [11], all these new bands can be ascribed to gypsum. Relating the disappearance of CAC to the formation of gypsum, this finding can be taken as evidence that the CAC has a strong chemical affinity with the H_2SO_4 to precipitate the gypsum. The spectral feature similar to that of the 80/20 ratio specimen was obtained from the 60/40, 40/60, and 20/80 ratio specimens, except for the presence of an additional band at 1061 cm^{-1}, belonging to the formation of $Ca(HPO_4).xH_2O$. There was no frequency band at 1428 cm^{-1}, originating from the calcite, inferring that the $CaCO_3$ may react with H_2SO_4 to generate gypsum and carbonic acid, $CaCO_3 + H_2SO_4 + 2H_2O \rightarrow CaSO_4.2H_2O + H_2CO_3$. Since a strong absorption band of $Ca(HPO_4).xH_2O$ at 1061 cm^{-1} still retains in the spectrum, it is reasonable to assume that the $Ca(HPO_4).xH_2O$ is less susceptibile to the reaction with H_2SO_4. The spectrum (not shown) also indicted the appearance of new bands at 3329 and 3096 cm^{-1}, corresponding to the O-H stretching in the γ-AlOOH, which was yielded by the phase transformation of amorphous $Al_2O_3.xH_2O$ gel. This finding strongly confirmed that the amorphous $Ca(HPO_4).xH_2O$ and $Al_2O_3.xH_2O$ gel reaction products play an essential role in minimizing the loss in weight of the specimens in a hot H_2SO_4 solution. On the other hand, once H_2SO_4 has attacked the CAC particles present in the hardened cement bodies, this acid preferentially reacts with the CA and CA_2 within the CAC to form the gypsum, rather than C_2AS. Hence, it is apparent that one of the factors governing the loss in weight can be accounted for leaching out of the water-soluble gypsum from the cement specimens during exposure. However, there are two other pieces of experimental evidence that must be considered: one is the fact that the degree of loss in weight was increasingly enhanced with an increasing ratio of fly ash/CAC; the other was that the *in-situ* growth of massive amounts of gypsum brought about by incorporating a large amount of CAC led to its lower degree. Therefore, the major cause for the serious damage to the specimens by H_2SO_4 attack is more likely to be associated with the development of porous structure of the specimens due to a substantial amount of unreacted fly ash remaining in the cements, rather than from the formation of gypsum. Numerous pores in a specimen not only lower its strength, but also allow the acid solution to permeate easily, diminishing the protection of the $Ca(HPO_4).xH_2O$ and $Al_2O_3.xH_2O$ gel phases against acid erosion.

This information was further supported by exploring the development of microstructure and inspecting the elemental composition of the fractured surfaces of exposed 80/20, 40/60, and 20/80 ratio specimens. Fig. 6 shows SEM micrographs, together with EDX spectra of these specimens. The intensity of a gross peak count of the EDX spectrum relates directly to the amount of respective element present. The morphological feature of the SEM image of the fly ash itself (not shown) represented a distribution of sphere-shaped particles with sizes ranging from approximately 0.1 to 10.0 μm. Furthermore, the accompanying EDX spectrum (not shown) had the three principal elements, oxygen, aluminum, and silicon, belonging to the mullite and quartz. The SEM images for all the specimens revealed the presence of unreacted spherical fly ash particles in the cement bodies. The microstructure of the 80/20 ratio specimen (top) was characterized by disclosing a very rough fracture surface and developing many propagating microcracks. Such a microtexture represented the disintegration of the cement by the attack of acid. The EDX spectrum taken from the site A indicates the elemental composition consisting of aluminum, silicon, sulfur, and calcium as the major elemental components, and oxygen, sodium, and phosphorous as minor ones. Assuming that two elements, Al and Si, from among these major components are ascribed to fly ash, the others, such as Ca and S, appear to arise mainly from gypsum. If such elucidation is valid, area A is explicable as the coverage of gypsum reaction products over the fly ash particles or their mix composites. From a weak signal of P, we judged that the formation of $Ca(HPO_4).xH_2O$, which arises from the interaction between CAC and NaP, is poorly developed in this cement system. In contrast, the SEM image of the 40/60 ratio specimen (middle) expressed a smooth fracture surface in conjunction with the generation of few microcracks, reflecting the development of a dense microstructure; this suggested that decreasing the ratio of fly ash to CAC contributed to altering the porous microtexture to a dense one. The EDX spectrum from the site B had six prominent

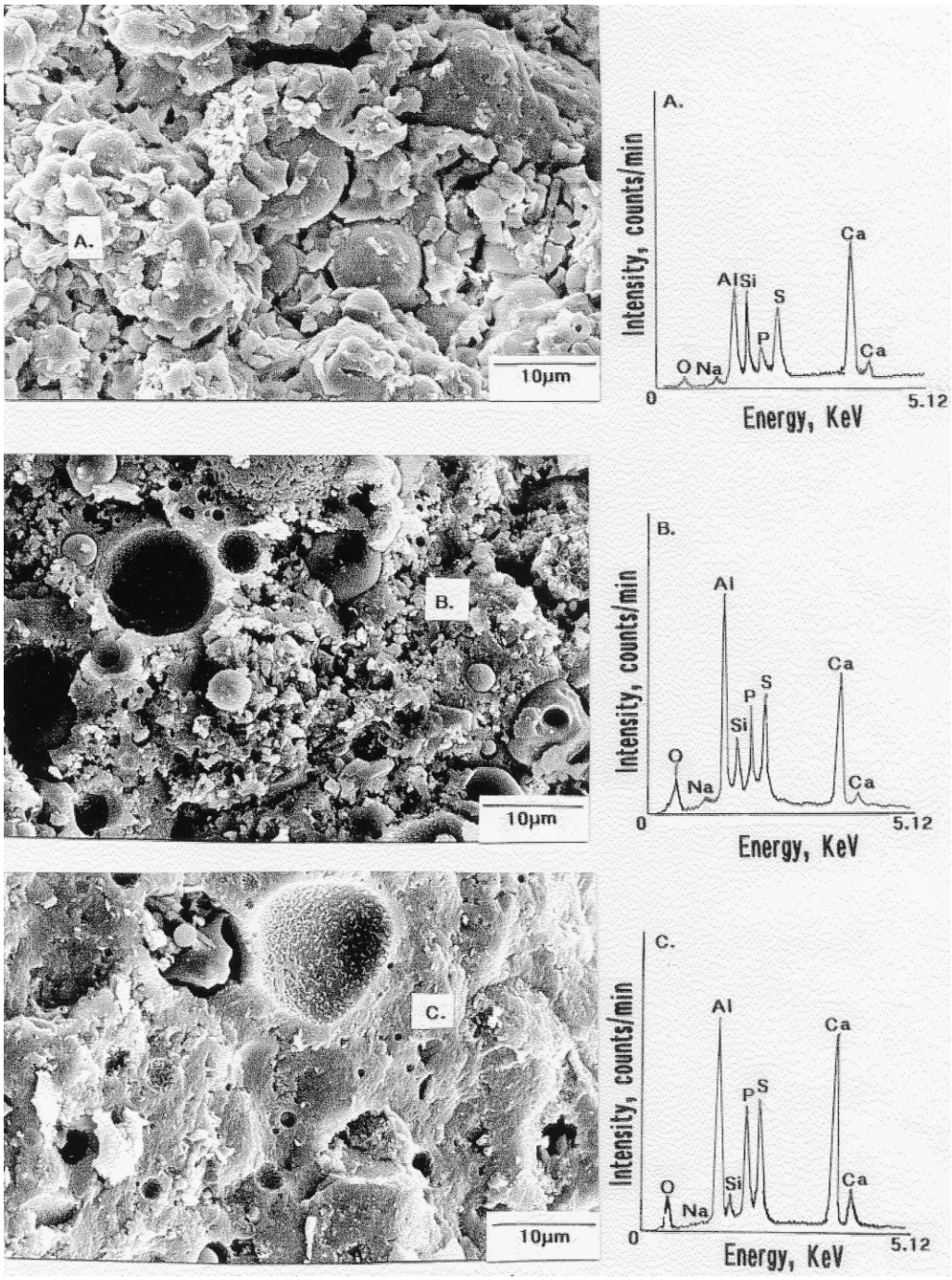

Fig. 6. Scanning electron micrographs coupled with EDX for fractured surfaces of (top) 80/20, (middle) 40/60, and (bottom) 20/80 ratio specimens after exposure to acid.

signals related to O, Al, Si, P, S, and Ca elements. Relating this to the XRD data, possible contributors to these elements include the three compounds, gypsum, $Ca(HPO_4).xH_2O$, and γ-AlOOH. Thus, the development of a dense microstructure might be due to the hybrid formation of these three compounds. Further densified microstructure can be seen in the SEM image of the 20/80 ratio specimens (bottom). The image also showed that the propagation of the fractures occurs along the surfaces of fly ash particles, but does not pass through their particles. Such a defect mode exemplifies that the reactivity of fly ash to NaP is very poor at low temperature of $<90°C$. The feature of the EDX spectrum at the site C was similar to that from the 40/60 ratio specimen, except for a lower intensity of the Si signal. Again, three reaction products, gypsum, $Ca(HPO_4).xH_2O$, and γ-AlOOH, were responsible for densifying the microstructure of the cement specimens after exposure to hot acid, offering improved mechanical behavior. In fact, the compressive strength of this

specimen was 24.5 MPa, corresponding to 1.4 times higher than that of the unexposed one.

4. Conclusions

Sodium polyphosphate-modified fly ash/calcium aluminate blend (SFCB) cements were prepared by mixing two cement-forming reactants, Class F fly ash-blending calcium aluminate cement as the solid reactant and 25 wt% sodium polyphosphate (NaP) solution as the liquid reactant, at room temperature, and then were exposed for up to 25 days to H_2SO_4 solution (pH 1.6) at 90°C. At room temperature, the NaP preferentially reacted with CAC to form amorphous $Ca(HPO_4).xH_2O$, rather than reacting with fly ash. Concurrently, such uptake of Ca in the CAC by NaP led to the formation of $Al_2O_3.xH_2O$ gel. Thus, the two reaction products, $Ca(HPO_4).xH_2O$ and $Al_2O_3.xH_2O$ gel, bound the partially reacted and unreacted CAC and fly ash particles into a substantial coherent mass, and also were responsible for strengthening and densifying the cement specimens. When the SFCB cements came in contact with hot acid solution, the gypsum was precipitated by the reaction between the H_2SO_4 and the two crystalline phases, monocalcium aluminate (CA) or calcium dialuminate (CA_2), present in the unreacted CAC particles. Furthermore, the decalcification of the CA and CA_2 by the acid also resulted in yielding the $Al_2O_3.xH_2O$ gel derivative, which was transformed into crystalline boehmite (γ-AlOOH) during exposure. The $Ca(HPO_4).xH_2O$ and $Al_2O_3.xH_2O$ gel showed little, if any susceptibility to the reaction with H_2SO_4, manifesting that these reaction products played an important role in mitigating acid erosion of the cement. The exposed specimens made with a lower ratio of fly ash/CAC included a substantial amount of hybrid phases consisting of $Ca(HPO_4).xH_2O$, gypsum, and γ-AlOOH, which aided in developing a densified microstructure of the cements and offering improved mechanical behavior. Although the formation of water-soluble gypsum was thought to be one of the factors governing the loss in weight of the cements, the major cause for serious acid erosion was the porous structure of the specimens brought about by a large amount of unreacted fly ash remaining in the cement, allowing acid solution to permeate easily and diminishing the protection offered by the $Ca(HPO_4).xH_2O$ and $Al_2O_3.xH_2O$ gel phases.

References

[1] T. Sugama, Hot alkali carbonation of sodium methaphosphate modified fly ash/calcium aluminate blend hydrothermal cements, Cem Concr Res 26(11) (1996) 1661–72.
[2] T. Sugama, Hydrothermal treatment of calcium aluminate-fly ash-sodium methaphosphate cements, Adv Cem Res 9(34) (1997) 65–73.
[3] L. Weber, E. Emersion, K. Harris, L. Brothers, The application of new corrosion resistant cement in geothermal wells. Geothermal Resources Council Transaction, September 20-23, San Diego, CA, 1998.
[4] F.G.R. Gimblett, Inorganic Polymer Chemistry, Butterworths, London, 1963.
[5] L.L. Hench, Bioceramic: from concept to clinic, J Am Ceram Soc 74(7) (1991) 1487–510.
[6] P.W. Brown, N. Hocker, S. Hoyle, Variations in solution chemistry during the low-temperature formation of hydroxyapatite, J Am Ceram Soc 74(8) (1991) 1848–54.
[7] M. Tanahashi, K. Kamiya, T. Suzuki, H. Hasu, Fibrous hydroxyapatite grown in the gel system: effect of pH of the solution on the growth rate and morphology, J Mater Sci: Materials in Medicine 3 (1992) 48–53.
[8] D.E.C. Carbridge, E.J. Lowe, J Chem Soc (1954) 493–502.
[9] L.J. Bellany, The Infra-red Spectra of Complex Molecules, Chapman and Hall, London, 1975.
[10] T. Sugama, M. Allen, J.M. Hill, Calcium phosphate cements prepared by acid-base reaction, J Am Ceram Soc 75(8) (1992) 2076–87.
[11] R.A. Nyquist, R.O. Kagel, Infrared Spectra of Inorganic Compounds, Academic Press, New York, 1971.